European Journal of Medicinal Chemistry 67 (2013) 196–207

Contents lists available at SciVerse ScienceDirect

European Journal of Medicinal Chemistry

journal homepage: http://www.elsevier.com/locate/ejmech

Original article

N-Aryl-6-methoxy-1,2,3,4-tetrahydroquinolines: A novel class of antitumor agents targeting the colchicine site on tubulin

Xiao-Feng Wang [a,c], Sheng-Biao Wang [a], Emika Ohkoshi [b], Li-Ting Wang [b], Ernest Hamel [d], Keduo Qian [b], Susan L. Morris-Natschke [b], Kuo-Hsiung Lee [b,e], Lan Xie [a,*]

[a] *Beijing Institute of Pharmacology & Toxicology, 27 Tai-Ping Road, Beijing 100850, China*
[b] *Natural Products Research Laboratories, UNC Eshelman School of Pharmacy, University of North Carolina at Chapel Hill, NC 27599, USA*
[c] *Pharmacy Department, Urumqi General Hospital, Lanzhou Military Region, Urumqi 830000, China*
[d] *Screening Technologies Branch, Developmental Therapeutics Program, Division of Cancer Treatment and Diagnosis, National Cancer Institute, Frederick National Laboratory for Cancer Research, National Institutes of Health, Frederick, MD 21702, USA*
[e] *Chinese Medicine Research and Development Center, China Medical University and Hospital, Taichung, Taiwan*

ARTICLE INFO

Article history:
Received 19 April 2013
Received in revised form
18 June 2013
Accepted 20 June 2013
Available online 29 June 2013

Keywords:
N-Aryl-6-methoxy-1,2,3,4-tetrahydroquinolines
Cytotoxicity
Tubulin polymerization inhibitors
Colchicine binding site

ABSTRACT

Structural optimizations of the prior lead **1a** led to the discovery of a series of *N*-aryl-6-methoxy-1,2,3,4-tetrahydroquinoline derivatives as a novel class of tubulin polymerization inhibitors targeted at the colchicine binding site. The most active compound **6d** showed extremely high cytotoxicity against a human tumor cell line panel (A549, KB, KBvin, and DU145) with GI_{50} values ranging from 1.5 to 1.7 nM, significantly more potent than paclitaxel, especially against the drug-resistant KBvin cell line, in the same assays. Analogs **5f**, **6b**, **6c**, and **6e** were also quite potent, with a GI_{50} range of 0.011–0.19 μM. In further studies, active compounds **6b**–**e** and **5f** significantly inhibited tubulin assembly, with IC_{50} values of 0.92–1.0 μM and strongly inhibited colchicine binding to tubulin, with inhibition rates of 75–99% (at 5 μM), comparable with or more potent than combretastatin A-4 (IC_{50} 0.96 μM). Current studies included design, synthesis, and biological evaluations of 24 new compounds (series **3**–**6**). Related SAR analysis, molecular modeling, and evaluation of essential drug-like properties, i.e. water solubility, log P, and *in vitro* metabolic stability, were also performed.

1. Introduction

Microtubules, formed by a dynamic polymerization and depolymerization of α- and β-tubulin heterodimers, play important roles in cellular activities [1]. For many years, certain drugs that bind to the taxol or vinca site on tubulin, such as paclitaxel and vinblastine, have been widely used in the clinic to treat cancers [2]. However, their narrow therapeutic windows and the emergence of drug resistance have encouraged continued efforts to discover safer and more effective agents capable of treating resistant cancer phenotypes. Another natural product colchicine (Fig. 1) binds to a unique site on tubulin, distinct from the above two binding sites, and can effectively inhibit tubulin assembly. Even though colchicine is not used clinically because of its high toxicity, other small molecules bind at the colchicine site, e.g., *N*-deacetyl-*N*-(2-mercaptoacetyl)-colchicine (DAMA–colchicine) and combretastatin A-4 (CA-4), and some have exhibited high potency, lower toxicity, and greater efficacy against cancers resistant to existing tubulin-targeting drugs [3]. More attractively, some of these compounds exhibit a vascular disrupting effect on vascular endothelial cells and have entered into clinical development as vascular disrupting agents (VDAs) for cancer treatment. Examples of this novel class of anticancer agents are CA-4P and ZD6126 (Fig. 1) [4,5].

In our prior studies on new anticancer agents [6,7], we discovered methyl 6-chloro-2-(*N*-(4-methoxyphenyl)-*N*-methyl)amino-nicotinate (**1a**, Fig. 2) as a lead compound with potent cytotoxic activity (GI_{50} 0.20–0.26 μM) against A549, KB, KBvin, and DU145 human tumor cell lines. Its biological target was identified as tubulin, specifically the colchicine site. Previous related SAR studies indicated that a *para*-methoxyphenyl moiety (B-ring) is an essential pharmacophore, that a tertiary amine linker can provide a feasible binding conformation, and that the substituted pyridine ring (A-ring) can be modified to improve potency. Based on these known SAR findings, we pursued optimization of lead **1a**, following the strategies shown in Fig. 2, to identify additional tubulin inhibitors with new scaffolds and high potency. Because the *o*-

* Corresponding author. Tel./fax: +86 10 6931690.
E-mail address: lanxieshi@yahoo.com (L. Xie).

0223-5234/$ – see front matter © 2013 Elsevier Masson SAS. All rights reserved.
http://dx.doi.org/10.1016/j.ejmech.2013.06.041

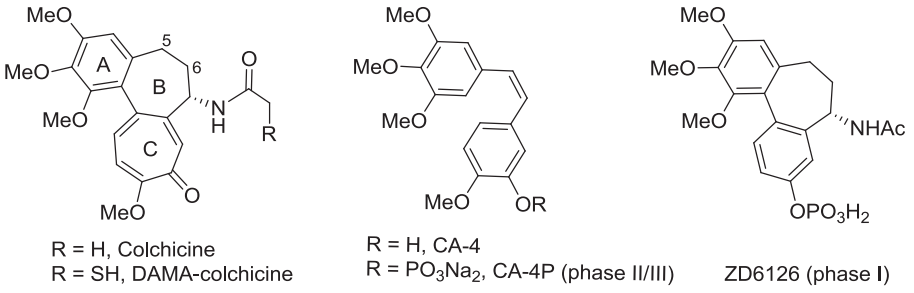

Fig. 1. Colchicine, DAMA–colchicine, and clinical trial candidates targeted at the colchicine site of tubulin.

chloropyridine moiety could potentially lead to metabolic toxicity resulting from *in vivo* nucleophilic replacement [8], we initially replaced the pyridine ring (A-ring) of **1a** with a benzene ring and also changed the identities and positions of substituents R^1 and X on the A-ring (series **3**–**4** compounds) to investigate how these modifications impacted inhibitory activity against tumor cell growth. Previously, we also postulated that the degree of torsional angle between the two aryl rings (A- and B-rings) might be crucial for activity; therefore, our next modification focused on the *N*-linkage. By applying a conformation restriction strategy [9], we connected a propyl group on the *N*-linker to the neighboring benzene ring (B-ring) to form a six-membered fused tetrahydropyridine ring (series **5** compounds). By constraining the flexible conformation, we could better explore feasible binding conformations and possible ligand–target interactions. We next postulated that introducing a fused aromatic ring onto the A-ring might make the molecular binding conformation of new series **6** compounds more similar to that of colchicine and enhance affinity with the binding site on tubulin, leading to better antitumor activity. All newly synthesized compounds were evaluated by cellular screening against a human tumor cell line (HTCL) panel, and selected potent compounds were also assayed for tubulin inhibition. Molecular modeling was used to illustrate the interaction between tubulin and the new ligand(s) as well as differences among ligands. Furthermore, certain essential parameters related to drug-like properties, such as water solubility, log P, and metabolic stability, were determined for highly potent compounds. Chemical synthesis, biological evaluation, molecular modeling, and SAR analysis are presented in this paper.

2. Chemistry

The syntheses of target compounds **3**–**6** are outlined in Schemes 1 and 2. Intermediate **2a** was prepared by Ullmann condensation reaction [10] of commercially available 4-methoxyaniline and 2,4-dichlorobenzoic acid in the presence of Cu/Cu_2O in 2-ethoxyethanol, following esterification with DMF–DMA (two equivalents) in toluene at reflux for 24 h. Intermediates **2b**–**d** were obtained by a Buchwald–Hartwig coupling reaction between 4-methoxyaniline and methyl 5-substituted-3-bromo (or iodo) benzoate in the presence of catalyst $Pd(OAc)_2$ and Cs_2CO_3 either with X-phos [11] under microwave (mw) irradiation at 120–150 °C (Method A for **2b** and **2c**) or with BINAP and traditional heating in toluene at reflux under nitrogen protection (Method B for **2d**). Subsequently, secondary amines **2a**–**d** were treated with methyl iodide in the presence of sodium hydride to afford corresponding tertiary diarylamines **3a** and **4a**–**c**. When using $LiAlH_4$ in THF at 0 °C for 1 h, the ester group of **3a** was reduced to a hydroxymethyl moiety, affording **3b** in nearly quantitative yield. Compound **3b** was further methylated with methyl iodide to give ether **3c**. Alternatively, the ester group in **3a** and **4a**–**c** was converted to an *N*-methylcarbamoyl group by treatment with methylamine in MeOH under mw irradiation at 100–120 °C to produce corresponding compounds **3d** and **4d**–**f**, respectively, in high yields (79–89%). Methylation of **4f** with methyl iodide yielded compound **4g** with a *N*,*N*-dimethylcarbamoyl group on the A-ring. Ester compound **4c** was hydrolyzed under basic conditions to produce carboxylic acid compound **4h**. Compound **4h** was then treated with 1-hydroxybenzotriazole (HOBt) in the presence of 1-ethyl-3-(3-dimethylaminopropyl)carbodiimide (EDCI) hydrochloride salt, followed by reaction with cyclopropylamine or cyclopentylamine to produce corresponding *N*-cyclopropylamide and *N*-cyclopentylamide compounds **4i** and **4j**, respectively [12]. By using Buchwald–Hartwig coupling reactions and the same conditions, compounds **5a**,**b** and **6a**,**b** were synthesized from intermediate 6-methoxy-1,2,3,4-tetrahydroquinoline (**7**) [13] and an aryl halide, such as phenyl, naphthyl, and quinolyl halides, in 68–75% yields. Similarly to series **3** and **4**, the ester group in **5a** and **5b** was converted into an *N*-alkylcarbamoyl or carboxy group to provide corresponding

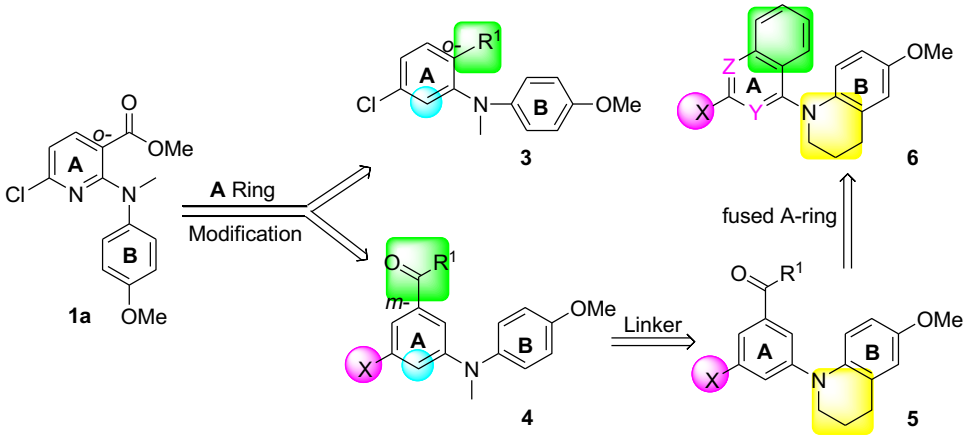

Fig. 2. Modification strategies and new target compounds **3**–**6** series.

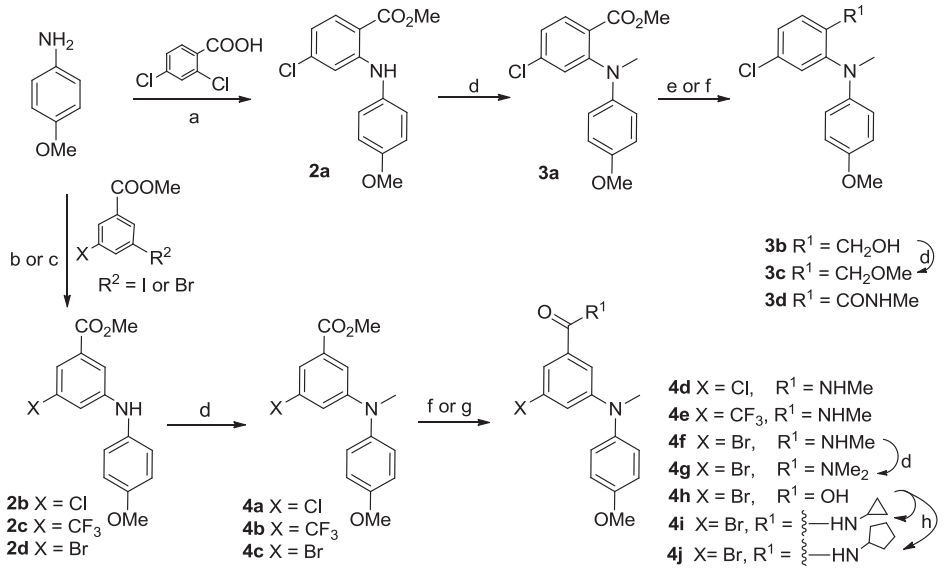

Scheme 1. a) i. K_2CO_3, Cu, Cu_2O, 2-ethoxyethanol, N_2, 130 °C, 24 h, 67%; ii. DMF–DMA in toluene, reflux, 2 h, 85%; b) i. Cs_2CO_3, $Pd(OAc)_2$, X-Phos, Celite, toluene/*t*-BuOH, N_2, mw, 120–150 °C, 30–60 min, 74% for **2b** and **2c**; c) Cs_2CO_3, $Pd(OAc)_2$, BINAP, toluene, N_2, reflux 12 h, 64% for **2d**; d) MeI/NaH (60% oil suspension), 0 °C, 1 h; e) $LiAlH_4$/THF, 0 °C, 1 h, 97%; f) 30% NH_2Me/MeOH, 100–120 °C, mw, 1–2 h for **3d**, **4d**–**f**; g) MeOH/THF, 3*N* NaOH aq, reflux, 5 h, 90% for **4h**; h) EDCI, HOBt, cyclopropylamine or cyclopentylamine, CH_2Cl_2, rt, 24 h for **4i** and **4j**.

compounds **5c**–**f** by using the same methods described above. Differently from **6a** and **6b**, the preparation of **6c** and **6d** involved coupling **7** with a 2-substituted 4-haloquinazoline under EtOH reflux in the presence of $NaHCO_3$, resulting in 79–87% yields. Using the same method for preparing **5c**, compound **6d** was converted to **6e**. All new series **3**–**6** compounds were identified by ^1H NMR and MS spectroscopic data, with purity determined by HPLC.

3. Results and discussion

3.1. Evaluation of cytotoxicity and tubulin inhibition activity in vitro

The 24 newly synthesized tertiary arylamines (series **3**–**6**) were evaluated in cellular cytotoxicity assays against a HTCL panel, including A549 (lung carcinoma), KB (epidermoid carcinoma of the mouth), KBvin, a P-gp-expressing multidrug-resistant cell line (vincristine-resistant KB) [14,15], and DU145 (prostate cancer) with paclitaxel as a reference compound. The *in vitro* anticancer activity (GI_{50}) was determined using the established sulforhodamine B (SRB) method [16]. The cytotoxicity data of all new compounds in HTCL assays are listed in Tables 1 and 2. Subsequently, selected compounds with high potency in cellular assays were further tested in tubulin assays to determine biological target and binding site.

In series **3** compounds with a phenyl A-ring and substituent X equal to *m*-chloro, two compounds **3a** (R^1 = *o*-COOMe) and **3c** (R^1 = *o*-CH_2OMe) showed promising potency with low micromolar GI_{50} values of 1.68–5.24 μM, indicating that replacement of the pyridine A-ring in lead **1a** is tolerated and R^1 on the A-ring is modifiable. When the COOMe group (R^1) was moved to the *meta*-position on the A-ring, the resulting compound **4a** exhibited

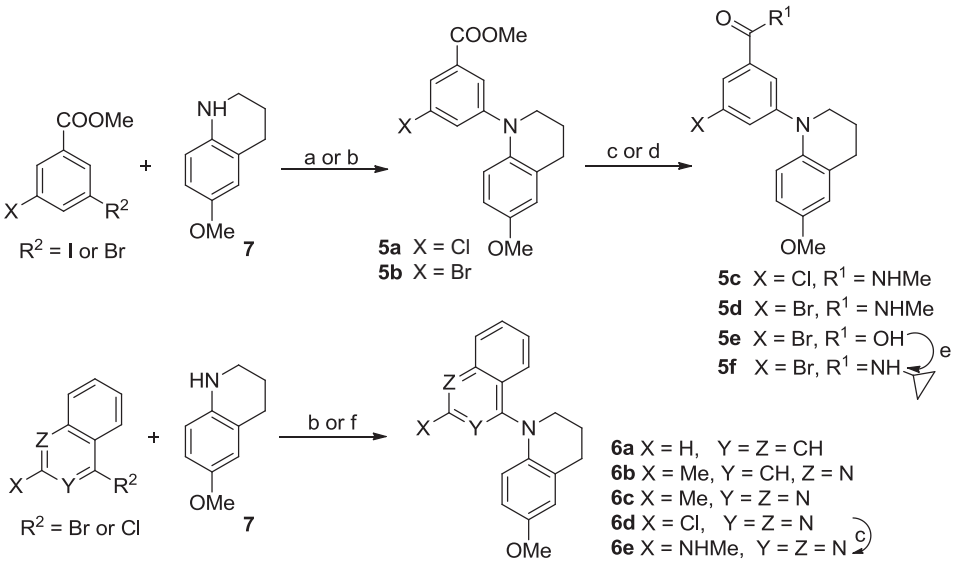

Scheme 2. a) Cs_2CO_3, $Pd(OAc)_2$, X-Phos, Celite, N_2, mw, 120 °C, 30 min, 77% for **5a**; b) Cs_2CO_3, $Pd(OAc)_2$, BINAP, toluene, N_2, reflux, 12 h, 68–75% for **5b** and **6a**,**b**; c) 30% NH_2Me/MeOH, 100 °C, mw, 1 h for **5c**, **5d**, and **6e**; d) MeOH/THF, 3 N NaOH aq, reflux, 5 h, 82% for **5e**; e) EDCI, HOBt, cyclopropylamine, CH_2Cl_2, rt, 24 h, 90%; f) $NaHCO_3$/EtOH, reflux, 3 h for **6c** and **6d**.

Table 1
Cytotoxicity of series **3**–**5** compounds against human tumor cell lines (HTCL).

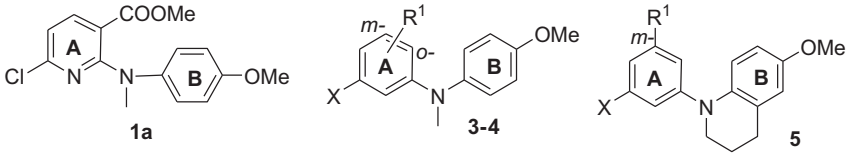

	X	R^1	GI_{50} (μM)[a]			
			A549	KB	KBvin	DU145
1a			0.23 ± 0.01	0.26 ± 0.04	0.20 ± 0.03	0.21 ± 0.04
3a	Cl	*o*-COOMe	3.36 ± 0.49	1.98 ± 0.37	1.89 ± 0.17	1.68 ± 0.04
3b	Cl	*o*-CH_2OH	21.7 ± 2.53	19.5 ± 1.33	18.1 ± 2.24	16.0 ± 2.73
3c	Cl	*o*-CH_2OMe	4.53 ± 0.84	5.24 ± 0.42	2.85 ± 0.62	3.13 ± 0.35
3d	Cl	*o*-CONHMe	43.2 ± 4.81	188 ± 33.8	61.0 ± 5.13	98.9 ± 4.22
4a	Cl	*m*-COOMe	1.60 ± 0.36	1.61 ± 0.08	1.57 ± 0.10	1.46 ± 0.16
4b	CF_3	*m*-COOMe	15.1 ± 2.6	13.5 ± 1.21	13.1 ± 1.41	11.5 ± 1.71
4c	Br	*m*-COOMe	1.24 ± 0.34	1.36 ± 0.17	1.20 ± 0.39	0.97 ± 0.08
4d	Cl	*m*-CONHMe	0.27 ± 0.01	0.30 ± 0.04	0.23 ± 0.04	0.23 ± 0.03
4e	CF_3	*m*-CONHMe	14.7 ± 2.23	12.3 ± 1.72	12.6 ± 1.81	11.9 ± 2.20
4f	Br	*m*-CONHMe	0.25 ± 0.07	0.21 ± 0.03	0.14 ± 0.01	0.16 ± 0.07
4g	Br	*m*-$CONMe_2$	2.83 ± 0.59	6.52 ± 1.16	2.38 ± 0.37	3.34 ± 0.54
4h	Br	*m*-COOH	NA[b]	NA	NA	NA
4i	Br	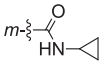	0.17 ± 0.02	0.17 ± 0.02	0.17 ± 0.02	0.17 ± 0.02
4j	Br	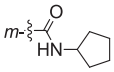	0.12 ± 0.02	0.12 ± 0.01	0.12 ± 0.01	0.11 ± 0.01
5a	Cl	*m*-COOMe	2.23 ± 0.23	2.33 ± 0.47	1.78 ± 0.31	1.51 ± 0.46
5b	Br	*m*-COOMe	1.12 ± 0.14	1.37 ± 0.31	1.27 ± 0.22	1.28 ± 0.25
5c	Cl	*m*-CONHMe	0.74 ± 0.08	1.04 ± 0.11	0.43 ± 0.03	1.02 ± 0.10
5d	Br	*m*-CONHMe	0.37 ± 0.08	0.63 ± 0.34	0.93 ± 0.02	0.56 ± 0.09
5f	Br	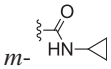	0.17 ± 0.01	0.16 ± 0.03	0.19 ± 0.01	0.15 ± 0.02
Paclitaxel[c]			0.0076 ± 0.0017	0.0064 ± 0.0014	1.21 ± 0.19	0.006 ± 0.001

[a] Concentration of compound that inhibits 50% human tumor cell growth, presented as mean ± standard deviation (SD), performed at least in triplicate.
[b] Not active; test compound (60 μM) did not reach 50% inhibition.
[c] Positive control.

somewhat improved activity (GI_{50} 1.46–1.61 μM) compared with **3a** (R^1 = *o*-COOMe, GI_{50} 1.68–3.36 μM). This finding prompted us to synthesize compounds **4b**–**f**, in which the *meta*-R^1 was either maintained as an ester (COOMe) or changed to a *N*-methylcarbamoyl (CONHMe) group, while substituent X was present as either a chloro, trifluoromethyl or bromo group. Interestingly, compounds **4a**, **4c**, **4d**, and **4f** where X is either chloride or bromide were more potent than **3a**. In addition, compounds **4d** and **4f** with a *meta*-*N*-methylcarbamoyl group (R^1) showed significantly improved potency with a GI_{50} range of 0.14–0.30 μM, compared with related *meta*-ester compounds **4a** and **4c**. In contrast, **4b** and **4e** with a trifluoromethyl (X) group were less active than corresponding chloro- and bromo-compounds in the same assays. Next, the cytotoxicity results for bromo-substituted compounds **4g**–**j** revealed the impact of the *m*-alkanoyl group (R^1). When the *meta*-*N*-methylcarbamoyl (**4f**) or *meta*-ester (**4c**) was converted to a more bulky *N*,*N*-dimethylcarbamoyl (**4g**) or more polar carboxy (**4f**) group, potency decreased or was abolished completely, respectively. But when R^1 was an *N*-cyclopropylcarbamoyl or *N*-cyclopentylcarbamoyl group, the corresponding compounds **4i** and **4j** showed improved potency with GI_{50} values of 0.11–0.17 μM, more potent than the other series **3** and **4** compounds, as well as **1a**. Because corresponding series **4** compounds (**4a**, **4d**) were more potent than series **3** compounds (**3a**, **3d**), we postulated that the *meta*-substitution on the A-ring might favor an appropriate torsional angle between the two aromatic rings, due to decreased steric hindrance around the *N*-linker, which would be consistent with our prior hypothesis. Moreover, the high potency of **4d**, **4f**, **4i**, and **4j** demonstrated that a hydrophobic *meta*-*N*-alkylcarbamoyl group with a suitable volume could enhance antitumor potency.

When the *N*-linker between the A- and B-rings was incorporated into a six-membered 1,2,3,4-tetrahydropyridine ring fused with the B-ring, all five compounds **5a**–**d**, **f** exhibited high cytotoxicity with GI_{50} values of 0.15–2.33 μM (Table 1). Thus, the ring-restricted *N*-linker was favorable for cytotoxic activity. Consequently, all series **6** compounds contain a 6-methoxy-1,2,3,4-tetrahydroquinoline moiety connected to an aromatic (naphthalene) or heteroaromatic (quinoline or quinazoline) bicyclic ring system, in which the resonance system of the A-ring is extended over an additional fused aromatic ring. As shown in Table 2, except for **6a** with a naphthyl A-ring system, compounds with either a quinoline (**6b**) or quinazoline (**6c**–**e**) moiety exhibited extremely high cytotoxicity in the HTCL assays. Among them, **6d** with a 2-chloroquinazoline moiety (A-ring) was the most potent with GI_{50} values ranging from 1.5 to 1.7 nM. Thus, **6d** was more potent than paclitaxel in the same assays, especially against the drug-resistant

Table 2
Cytotoxicity of **6** series against human tumor cell lines.

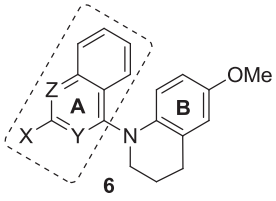

6

	Fused A-ring			GI_{50} (μM)[a]			
	X	Y	Z	A549	KB	KBvin	DU145
6a	H	CH	CH	17.8 ± 2.6	15.6 ± 1.3	17.6 ± 2.5	14.8 ± 1.7
6b	Me	CH	N	0.045 ± 0.008	0.091 ± 0.009	0.055 ± 0.010	0.038 ± 0.008
6c	Me	N	N	0.018 ± 0.001	0.011 ± 0.001	0.018 ± 0.004	0.015 ± 0.005
6d	Cl	N	N	0.0017 ± 0.0003	0.0017 ± 0.0008	0.0017 ± 0.0003	0.0015 ± 0.0003
6e	NHMe	N	N	0.027 ± 0.005	0.025 ± 0.002	0.029 ± 0.005	0.023 ± 0.003
Paclitaxel[b]				0.0076 ± 0.0017	0.0064 ± 0.0014	1.21 ± 0.19	0.006 ± 0.001

[a] Concentration of compound that inhibits 50% human tumor cell growth.
[b] Positive control.

KBvin cell line (GI_{50} 0.0017 μM versus 1.21 μM, respectively). Compounds **6b** (2-methylquinoline), **6c** (2-methylquinazoline), and **6e** (2-methylaminoquinazoline) also showed high cytotoxicity with a GI_{50} range of 11–91 nM, more potent by at least ten-fold than **1a** and series **3**–**5** compounds. Similarly to **6d**, analogs **6b**, **6c**, and **6e** were also much more potent than paclitaxel against KBvin cell growth, indicating that this compound type has great potential to overcome resistance to paclitaxel.

Based on these results in cellular assays, active compounds **4f**, **4i**, **5f**, and **6b**–**e** (GI_{50} < 1 μM) were evaluated in tubulin inhibition assays, in parallel with CA-4, a drug candidate in clinical trials, as a reference. As shown in Table 3, while *N*-methyl linked compounds **4f** and **4i** (open *N*-linker) showed good inhibitory potency against tubulin assembly (IC_{50} 1.6–2.2 μM), the *N*-phenyl-6-methoxy-1,2,3,4-tetrahydroquinoline compound **5f** (ring-restricted *N*-linker) exhibited improved potency in both tubulin assembly (IC_{50} 1.0 μM) and colchicine binding (75%) assays. Thus, the presence of the ring-restricted *N*-linker probably increases compound affinity for tubulin. Furthermore, **6b**–**e** with both a ring-restricted *N*-linker and a fused bicyclic aromatic ring system (A-ring) also displayed high potency in the tubulin assembly (IC_{50} 0.92–1.00 μM) and inhibition of colchicine binding (87–99% at 5 μM and 61–95% at 1 μM) assays, comparable with and greater than those of **5f**, respectively. Consistent with the cellular assays, compound **6d** was the most potent compound with an IC_{50} value of 0.93 μM against tubulin assembly and inhibitory rates of 99% and 95% at 5 μM and 1 μM, respectively, for competitively inhibiting colchicine binding to tubulin. These data are comparable or better than those for the reference compound CA-4 (IC_{50} 0.96 μM, 98% and 90% respectively). Thus, *N*-aryl-6-methoxy-1,2,3,4-tetrahydroquinoline compounds, e.g., series **5**–**6**, likely present a novel class of highly potent tubulin polymerization inhibitors targeted at the colchicine binding site. Meanwhile, we postulated that a fused bicyclic aromatic A-ring might interact with the colchicine site in some way, possibly resulting in increased affinity for tubulin. On the other hand, the active **6** series compounds might also interact with other unidentified target(s), because **6b**–**e** displayed much higher potency than **5f** in the cellular cytotoxicity assays, but similar inhibitory activity against tubulin polymerization.

Table 3
Inhibition of tubulin polymerization[a] and colchicine binding to tubulin.[b]

Compound	Inhibition of tubulin assembly IC_{50} (μM) ± SD	Inhibition of colchicine binding (%) inhibition ± SD	
		At 5 μM	At 1 μM
4f	2.2 ± 0.2	71 ± 0.3	ND[c]
4i	1.6 ± 0.04	69 ± 3.0	ND
5f	1.0 ± 0.1	75 ± 1.0	ND
6b	1.0 ± 0.1	87 ± 2.0	61 ± 2.0
6c	1.0 ± 0.1	98 ± 0.2	89 ± 2.0
6d	0.93 ± 0.04	99 ± 0.6	95 ± 0.7
6e	0.92 ± 0.06	95 ± 0.2	76 ± 0.1
CA4[d]	0.96 ± 0.07	98 ± 0.6	90 ± 0.2

[a] The tubulin assembly assay measured the extent of assembly of 10 μM tubulin after 20 min at 30 °C.
[b] Tubulin: 1 μM. [^{3}H]colchicine: 5 μM. Inhibitor: 5 μM or 1 μM (compounds inhibiting colchicine binding by more than 80% at 5 μM were further tested). Incubation was performed for 10 min at 37 °C.
[c] Not determined.
[d] Reference compound is a drug candidate in phase II/III clinical trials.

3.2. Molecular modeling

To better understand interactions between the newly synthesized active inhibitors and tubulin, we investigated potential binding modes of active compounds **4i**, **5f**, and **6d** at the colchicine site in the tubulin dimer by using the CDOCKER program in the Discovery Studio 3.0 software with the tubulin crystal structure (PDB: 1SA0) [17,18], as in our previous study. In the binding models shown in Fig. 3A, both **4i** (purple) and **5f** (green) displayed low energy binding conformations (−30.58 and −33.31 kcal/mol, respectively) that superimposed well with each other and with DAMA–colchicine (cyan), the ligand used in the tubulin crystal structure. As seen in Fig. 3A, a hydrogen bond is present between Val181 in the α-T5 loop of tubulin and the amide carbonyl group on the A ring of **4i** and **5f**. This hydrogen bond is also observed between Val181 and the carbonyl group on the C-ring of DAMA–colchicine. In addition, the *N*-cyclopropyl of the amide group in both **4i** and **5f** overlaps with the methoxy group on the seven-membered ring (C-ring) of DAMA–colchicine and stretches into a small lipophilic pocket around the amino acids in α-T5, β-H8, β-S8 and β-S9 of tubulin. In addition, the 4-methoxyphenyl moiety (B-ring) in **4i** and **5f**, regardless of whether the *N*-linker is open or ring-restricted, overlaps with the trimethoxyphenyl portion of DAMA–colchicine. The 4-OCH_3 group on the B-ring of **4i** and **5f** forms a hydrogen bond with the Cys241 side chain in β-H7 of tubulin, and a similar interaction is also observed with the 2′-OCH_3

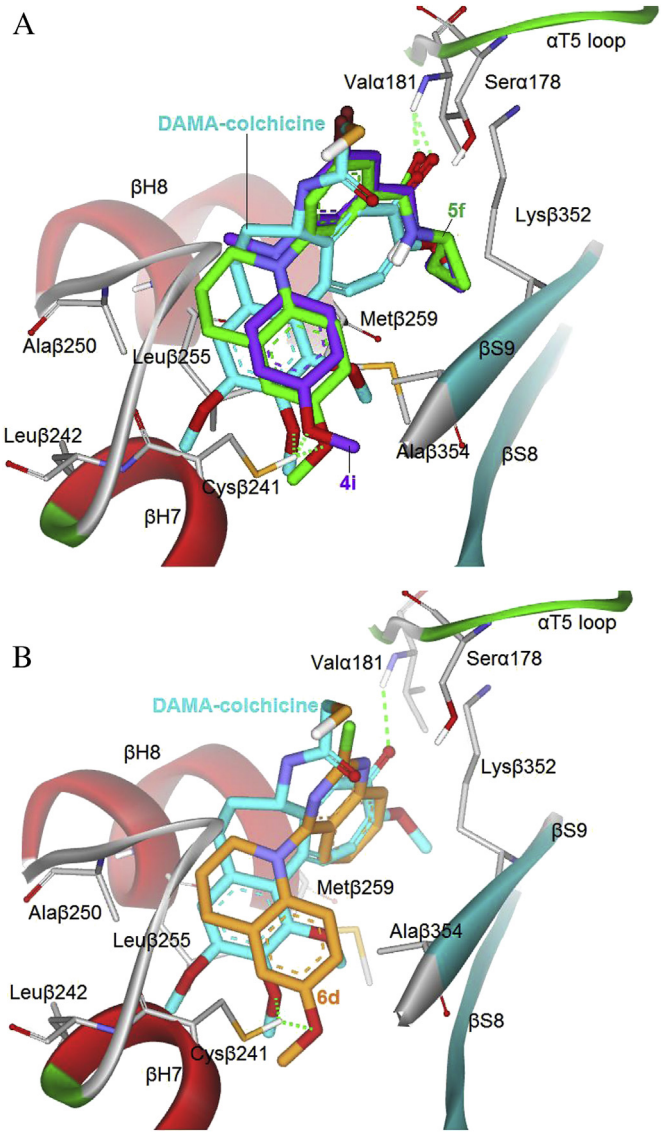

Fig. 3. (A) Predicted modes for **4i** (purple stick) and **5f** (green) binding with tubulin (PDB code: 1SA0), and overlapping with DAMA–colchicine (cyan, the native ligand of 1SA0); (B) Superimposition of docked compound **6d** (orange) with DAMA–colchicine (cyan). Surrounding amino acid side chains are shown in gray stick format and labeled. Hydrogen bonds are shown by green dashed lines, and the distance between ligands and protein is less than 3 Å. (For interpretation of the references to color in this figure legend, the reader is referred to the web version of this article.)

on the A-ring of DAMA–colchicine. Cys241 is a key amino acid that interacts with most tubulin inhibitors bound at the colchicine site. In the crystal structure, the C5 and C6 atoms of the B-ring of DAMA–colchicine are involved in hydrophobic interactions with the side chains of Alaβ250 and Leuβ255 in tubulin's β-H8 region. Although the *N*–CH_3 linker in **4i** is not in close proximity to Alaβ250 and Leuβ255 (>4 Å), the added carbons in the six-membered tetrahydropyridine cyclic linker in **5f** are closer to the hydrophobic side chains of Alaβ250 and Leuβ255 (<4 Å). The additional van der Waal's force between the cyclic linker and the binding site would likely strengthen affinity of **5f** for tubulin. Therefore, our current modeling results might explain, at least partially, the higher potency of **5f** than **4f** and **4i** in the tubulin assays (Table 3).

Consistent with our earlier hypothesis [6,7], the steric hindrance of the *N*–CH_3 linker [19] results in a binding torsional angle of 74.89° between the two aromatic rings in **4i**, allowing the *N*-alkyl amide group on the A-ring to interact with the binding site as described above. When the *N*-linker is connected with additional carbons into a six-membered ring, a similar torsional angle (70.52°) was found, maintaining a favorable binding conformation for **5f** and all major interactions with the binding site as mentioned above for **4i**. Fig. 3B shows that **6d** (binding energy: −34.39 kcal/mol) has a similar binding orientation as those of **4i** and **5f**, as well as good superimposition with DAMA–colchicine. The major interactions of the B-ring and the cyclic linker with tubulin are maintained. The torsional angle (69.07°) between the two rings in **6d** is similar to that of **5f**, resulting in a superimposition between the quinazoline ring of **6d** and the aromatic C-ring of DAMA–colchicine. Although we postulated that the fused aromatic ring introduced in **6d** would play a role similar to that of the C-ring of colchicine within the binding site on tubulin, no interaction was obvious in the computational model. Because of the torsional angle between the two aryl rings, the 2-chloro group on the quinazoline in **6d** [as well as the *m*-bromo group on the phenyl (A-ring) in **4i** and **5f** (Fig. 3A)] was orientated similarly to the acetyl group on the B-ring in DAMA–colchicine. Thus, the X substituent on the quinazoline (or other aromatic ring system) might interact with tubulin in some way and be modifiable.

3.3. Drug-like property evaluations

Next, we evaluated aqueous solubility and log P parameters of **4f**, **4i**, **5f**, and **6b**–**e** as described previously [20]. As shown in Table 4, compounds **6b**, **6c**, and **6e** showed much better aqueous solubility (3.21–7.67 μg/mL) than the other four compounds (<1.0 μg/mL). Consistently, log P values of **6b**, **6c**, and **6e** (1.07–3.98) were also lower (**4f**, **4i**, **5f**, **6d** > 4). Subsequently, metabolic stability of **6b**–**e** was further evaluated by an *in vitro* human liver microsome incubation assay with propranolol (moderate metabolism *in vivo*, $t_{1/2}$ 3–5 h) and terfenadine (fast metabolism *in vivo*, $t_{1/2}$ < 3 h) as positive controls. Compounds **6c** ($t_{1/2}$ 25.19 min) and **6e** ($t_{1/2}$ 25.97 min) were more stable than terfenadine ($t_{1/2}$ 21.14), while **6b** and **6d** were even less stable with short metabolic half-lives of 7.89 min and 10.59 min, respectively, indicating quick metabolism. In general, a potent compound with low metabolic stability is not usually recognized as a promising drug candidate. However, compounds targeting the colchicine site of tubulin are proposed as VDAs to treat cancers. For this new type of anticancer drug candidate, rapid metabolism might be desirable to decrease drug toxicity in the body, as exemplified by ZD6126 (Fig. 1), which was developed based on this hypothesis [21].

Table 4
Physicochemical parameters of selected compounds.

Compound	At pH 7.4		Human liver microsome $t_{1/2}$ min
	Water solubility (μg/mL)	Log P	
4f	0.81 ± 0.01	4.02 ± 0.11	ND[c]
4i	0.16 ± 0.03	4.33 ± 0.12	ND
5f	0.26 ± 0.05	4.75 ± 0.09	ND
6b	3.21 ± 0.60	3.98 ± 0.02	7.89
6c	7.67 ± 0.40	3.65 ± 0.03	25.19
6d	0.45 ± 0.06	4.13 ± 0.05	10.59
6e	7.21 ± 0.06	1.07 ± 0.21	25.97
Propranolol[a]			40.82
Terfenadine[b]			21.14

Data presented as mean from three separate experiments with or without ± standard deviation (SD).
[a] Propranolol has moderate metabolic stability with $t_{1/2}$ of 3–5 h *in vivo*.
[b] Terfenadine has fast metabolic stability with $t_{1/2}$ of <3 h *in vivo*.
[c] Not determined.

4. Conclusion

Modifications of prior lead **1a** resulted in the synthesis and biological evaluation of 24 new compounds (series **3**–**6**). During this process, active compound **6d** showed extremely high cytotoxicity against the screening HTCL panel with a GI_{50} value range of 1.5–1.7 nM, more potent than paclitaxel in the same assays, especially against resistant KBvin. Compound **6d** also displayed significant inhibitory activity in tubulin assembly (IC_{50} 0.93 μM) and colchicine binding (inhibition 99% at 5 μM and 95% at 1 μM) assays, with greater potency than CA-4. Similarly, analogs **6b**, **6c**, and **6e** also showed high potency in the cellular (GI_{50} 11–91 nM) and tubulin (IC_{50} 0.92–1.0 μM) assays. Therefore, *N*-aryl-6-methoxy-1,2,3,4-tetrahydroquinoline derivatives were identified as a novel class of tubulin polymerization inhibitors targeted at the colchicine site. Current SAR studies lead to the following conclusions: (1) a ring-restricted *N*-linker is beneficial and provides a feasible torsional angle (about 70–75°) between the two aryl ring systems (A and B rings) for enhancing molecular affinity for tubulin; (2) the 6-methoxy-1,2,3,4-tetrahydroquinoline moiety can serve as a pharmacophore and the methoxy group on the B-ring is a necessary binding point to tubulin; (3) isosteric replacement of the A-ring is feasible and a fused aromatic ring, such as quinoline and quinazoline, improved molecular potency; (4) various *m*-substituents on the A-ring are present in active compounds, and either halogen or *N*-alkyl amide/amino might be beneficial. Molecular modeling results illustrated some possible interactions of the active compounds with the colchicine site of tubulin and supported our earlier hypothesis that a feasible torsional angle between the two aryl rings might be important for high potency. An evaluation of essential drug-like properties, i.e. water solubility, log P, and metabolic stability *in vitro*, also provided useful information. These results will help us to develop drug candidates from this novel class of tubulin inhibitors targeted at the colchicine site in further studies.

5. Experimental section

5.1. Chemistry

Proton and carbon nuclear magnetic resonance (^1H and ^{13}C NMR) spectra were measured on a JNM-ECA-400 (400 MHz) spectrometer using tetramethylsilane (TMS) as internal standard. The solvent used was $CDCl_3$ unless otherwise indicated. Mass spectra (MS) were measured on an API-150 mass spectrometer with an electrospray ionization source from ABI, Inc. Melting points were measured by a SGW X-4 Micro-Melting point detector without correction. The mw reactions were performed on a mw reactor from Biotage, Inc. Medium-pressure column chromatography was performed using a CombiFlash® Companion system from ISCO, Inc. Thin-layer chromatography (TLC) was performed on silica gel GF254 plates. Silica gel GF254 and H (200–300 mesh) from Qingdao Haiyang Chemical Company were used for TLC and column chromatography, respectively. All commercial chemical reagents were purchased from Beijing Chemical Works or Sigma–Aldrich, Inc. Reagents NADPH, $MgCl_2$, KH_2PO_4, K_2HPO_4, and reference compounds propranolol and terfenadine were purchased from Sigma–Aldrich. HPLC grade acetonitrile for LC–MS analysis was purchased from VWR. Pooled human liver microsomes (lot no. 28831) were purchased from BD Biosciences (Woburn, MA). Purities of target compounds were determined by using an Agilent HPLC-1200 with UV detector and an Agilent Eclipse XDB-C18 column (150 mm × 4.6 mm, 5 μm), flow rate 0.8 mL/min, UV detection at 254 nm, and injection volume of 15 μL. Mobile elution was conducted with a mixture of solvents A and B [Condition 1: acetonitrile (ACN)/water 60–80/40–20; Condition 2: MeOH/water 70–90/30–10]. For **6b**, **6c** and **6e**, solvent B contained 0.025 mM ammonium acetate.

5.1.1. Methyl 4-chloro-2-(4-methoxyphenyl)aminobenzoate (*2a*)

A mixture of 2,4-dichlorobenzoic acid (1.91 g, 10 mmol), 4-methoxyaniline (1.29 g, 10.5 mmol), copper powder (58 mg, 9% mmol), cuprous oxide (58 mg, 4% mmol), anhydrous potassium carbonate (1.38 g, 10 mmol) and 2-ethoxyethanol (7.5 mL) was refluxed under N_2 protection for 24 h with stirring. The mixture was poured into water and active carbon added. After filtration through Celite, the filtrate was adjusted to pH 3–4 with aq HCl. The collected gray solid was dried to obtain 1.85 g of 4-chloro-2-(4-methoxyphenyl) aminobenzoic acid (0.83 g, 3.0 mmol), which was methylated directly with DMF–DMA (0.79 mL, 6.0 mmol) in toluene (12 mL) under reflux for 2 h. After removal of solvent *in vacuo*, the residue was purified by flash column chromatography (gradient elution: EtOAc/petroleum ether, 0–30%) to obtain 0.74 g of **2a** in a 57% yield over two steps. It was used next without further purification.

5.1.2. Methyl 3-chloro-5-(4-methoxyphenylamino)benzoate (*2b*)

A mixture of methyl 3-chloro-5-iodobenzoate (296 mg, 1.0 mmol), 4-methoxyaniline (148 mg, 1.2 mmol), Cs_2CO_3 (455 mg, 1.4 mmol), X-Phos (17 mg, 0.04 mmol), $Pd(OAc)_2$ (11 mg, 0.05 mmol), Celite (228 mg), and *t*-BuOH (0.5 mL) in toluene (3 mL) was heated at 120 °C for 1 h under mw irradiation with stirring. EtOAc (10 mL) was added to the mixture, and, after brief stirring, insoluble solid was removed by filtration. After removal of organic solvent *in vacuo*, the residue was purified by flash column chromatography (gradient elution: EtOAc/petroleum ether, 0–40%) to obtain **2b** as a yellow solid, 216 mg, 74% yield, which was used directly in the next step without further purification.

5.1.3. Methyl 3-trifluoromethyl-5-(4-methoxyphenylamino) benzoate (*2c*)

A mixture of methyl 3-trifluoromethyl-5-bromobenzoate (285 mg, 1.0 mmol), 4-methoxyaniline (147 mg, 1.2 mmol), Cs_2CO_3 (455 mg, 1.4 mmol), X-Phos (17 mg, 0.04 mmol), $Pd(OAc)_2$ (11 mg, 0.05 mmol), Celite (228 mg), and *t*-BuOH (0.5 mL) in toluene (3.0 mL) was heated at 150 °C for 30 min under mw irradiation. After work-up as for **2b**, 240 mg of **2c** was obtained in 74% yield, yellow solid, which was directly used for the next step without further purification.

5.1.4. Methyl 3-bromo-5-(4-methoxyphenylamino)benzoate (*2d*)

A mixture of methyl 3,5-dibromobenzoate (294 mg, 1.0 mmol), 4-methoxyaniline (146 mg, 1.2 mmol), Cs_2CO_3 (455 mg, 1.4 mmol), BINAP (31 mg, 0.05 mmol), and $Pd(OAc)_2$ (11 mg, 0.05 mmol) in toluene (5–10 mL) was refluxed for 12 h under nitrogen protection. After the mixture was cooled to rt, EtOAc (10 mL) was added. After stirring, the insoluble material was removed by filtration. The solvent was removed *in vacuo*, and the residue was purified by flash column chromatography (gradient elution: EtOAc/petroleum ether, 0–40%) to produce 215 mg of **2d** in 64% yield as a brown oil.

5.1.5. General procedure for methylation of aniline NH with methyl iodide to prepare *3a* and *4a–c*

To a solution of a diarylamine (**2**) and MeI (molar ratio: 1/2–3) in anhydrous DMF (ca. 3 mL) was slowly added NaH (2–3 equiv, 60% oil suspension) at 0 °C with stirring over about 1 h. When the reaction was completed as monitored by TLC, the mixture was poured into ice-water and extracted with EtOAc three times. The combined organic phase was washed with water and brine successively and dried over anhydrous Na_2SO_4 overnight. After removal of solvent *in vacuo*, the crude product was purified by flash column chromatography (gradient elution: EtOAc/petroleum ether,

0–50%) to give the corresponding methylated tertiary amine compounds.

*5.1.5.1. Methyl 4-chloro-2-(N-(4-methoxyphenyl)-N-methylamino) benzoate (**3a**).* Starting with **2a** (670 mg, 2.3 mmol), methyl iodide (0.28 mL, 4.6 mmol) and NaH (184 mg, 4.6 mmol) to produce 662 mg of **3a** in 82% yield, yellow solid, mp 52–53 °C; ^{1}H NMR δ ppm 3.27 (3H, s, NCH_3), 3.51 (3H, s, OCH_3), 3.76 (3H, s, OCH_3), 6.80 (4H, m, ArH-2′,3′,5′,6′), 7.02 (1H, dd, J = 8.4 and 2.0 Hz, ArH-5), 7.15 (1H, d, J = 2.0 Hz, ArH-3), 7.55 (1H, d, J = 8.0, ArH-6); MS m/z (%) 306 (M + 1, 100), 308 (M + 3, 26); HPLC purity 98.3%.

*5.1.5.2. Methyl 3-chloro-5-(N-(4-methoxyphenyl)-N-methylamino) benzoate (**4a**).* Starting with **2b** (322 mg, 1.1 mmol), methyl iodide (0.14 mL, 2.2 mmol) and NaH (88 mg, 2.2 mmol) to produce 328 mg of **4a** in 98% yield, yellow solid, mp 58–60 °C; ^{1}H NMR δ ppm 3.27 (3H, s, NCH_3), 3.84 (3H, s, OCH_3), 3.87 (3H, s, OCH_3), 7.04 (1H, t, J = 2.0 Hz, ArH-2), 6.94 (2H, d, J = 8.8 Hz, ArH-2′,6′), 7.10 (2H, d, J = 8.8 Hz, ArH-3′,5′), 7.26 (1H, m, ArH-4), 7.35 (1H, t, J = 2.0 Hz, ArH-6). MS m/z (%) 306 (M + 1, 39), 308 (M + 3, 13), 291 (100); HPLC purity 99.3%.

*5.1.5.3. Methyl 3-trifluoromethyl-5-(N-(4-methoxyphenyl)-N-methylamino)benzoate (**4b**).* Starting with **2c** (188 mg, 0.58 mmol), methyl iodide (0.07 mL, 1.2 mmol), and NaH (48 mg, 1.2 mmol) to produce 176 mg of **4c** in 89% yield, yellow oil; ^{1}H NMR δ ppm 3.32 (3H, s, NCH_3), 3.85 (3H, s, OCH_3), 3.90 (3H, s, OCH_3), 6.95 (2H, d, J = 8.8 Hz, ArH-2′,6′), 7.04 (1H, s, ArH-2), 7.12 (2H, d, J = 8.8 Hz, ArH-3′,5′), 7.51 (1H, s, ArH-4), 7.61 (1H, s, ArH-6). MS m/z (%) 340 (M + 1, 55), 325 (M − 14, 100); HPLC purity 98.7%.

*5.1.5.4. Methyl 3-bromo-(N-(4-methoxyphenyl)-N-methylamino) benzoate (**4c**).* Starting with **2d** (128 mg, 0.38 mmol), methyl iodide (0.07 mL, 1.1 mmol) and sodium hydride (44 mg, 1.1 mmol) to produce 115 mg of **4c** in 90% yield, yellow oil; ^{1}H NMR δ ppm 3.27 (3H, s, NCH_3), 3.84 (3H, s, OCH_3), 3.87 (3H, s, OCH_3), 6.94 (3H, m, ArH-2,2′,6′), 7.10 (2H, d, J = 8.8 Hz, ArH-3′,5′), 7.29 (1H, m, ArH-4), 7.50 (1H, s, ArH-6). MS m/z (%) 350 (M + 1, 34), 352 (M + 3, 29), 337 (M − 14, 100); HPLC purity 95.0%.

*5.1.6. 5-Chloro-2-hydroxymethyl-N-(4-methoxy)phenyl-N-methylaniline (**3b**)*

A solution of **3a** (427 mg, 1.40 mmol) in THF (4 mL) was added dropwise to $LiAlH_4$ (108 mg, 2.89 mmol, excess) in anhydrous THF (5 mL) at 0 °C with stirring, which was continued at the same temperature for another 1 h. After the reaction was complete, as monitored by TLC, to the mixture was added 0.11 mL of water, 0.33 mL of 15% aq NaOH, and 0.33 mL of water, successively, with stirring for another 10 min at rt. Then the mixture was filtered through Celite, solvent was removed *in vacuo*, and the residue was purified by flash column chromatography (gradient elution: EtOAc/petroleum ether 0–40%) to produce 377 mg of **3b** in 97% yield, brown oil; ^{1}H NMR δ ppm 3.19 (3H, s, NCH_3), 3.76 (3H, s, OCH_3), 4.48 (2H, s, OCH_2), 6.68 (2H, d, J = 9.2 Hz, ArH-2′,6′), 6.79 (2H, d, J = 9.2 Hz, ArH-3′,5′), 7.12 (1H, d, J = 2.0 Hz, ArH-3), 7.19 (1H, dd, J = 8.0 & 2.0 Hz, ArH-5), 7.38 (1H, d, J = 8.0, ArH-6). MS m/z (%) 278 (M + 1, 100), 280 (M + 3, 36).

*5.1.7. 5-Chloro-2-(methoxymethyl)-N-(4-methoxy)phenyl-N-methylaniline (**3c**)*

Prepared in the same manner as for **3a**, starting with **3b** (227 mg, 0.82 mmol), methyl iodide (0.10 mL, 1.6 mmol), and NaH (66 mg, 1.6 mmol) to produce 228 mg of **3c** in 95% yield, yellow oil; ^{1}H NMR δ ppm 3.17 (3H, s, NCH_3), 3.32 (3H, s, OCH_3), 3.76 (3H, s, OCH_3), 4.26 (2H, s, OCH_2), 6.60 (2H, d, J = 9.2 Hz, ArH-2′,6′), 6.79 (2H, d, J = 9.2 Hz, ArH-3′,5′), 7.11 (1H, d, J = 2.0 Hz, ArH-3), 7.20 (1H, dd, J = 8.4 & 2.0 Hz, ArH-5), 7.45 (1H, d, J = 8.4, ArH-6). MS m/z (%) 292 (M + 1, 22), 294 (M + 3, 7), 228 (M − 63, 100).

*5.1.8. General procedure for preparing N-methylamides **3d**, **4d**–**f** from esters under mw irradiation*

A solution of ester compound (0.17 mmol–0.40 mmol) in 3 mL 30% methylamine in MeOH was heated to 100–120 °C under mw irradiation for 1–2 h. Then the mixture was poured into ice-water, neutralized with aq HCl (2 N), and extracted with EtOAc three times. The combined organic phase was washed with water and brine, successively, and dried over anhydrous Na_2SO_4 overnight. After removal of solvent *in vacuo*, the crude product was purified by flash column chromatography (gradient elution: EtOAc/petroleum ether, 0–70%) to give the corresponding target compound.

*5.1.8.1. N-Methyl-4-chloro-2-(N-(4-methoxy)phenyl-N-methylamino)benzamide (**3d**).* Starting with **3a** (115 mg, 0.38 mmol) at 120 °C for 2 h to produce 92 mg of **3d**, 79% yield, yellow oil; ^{1}H NMR δ ppm 2.89 (3H, d, J = 5.2 Hz, NCH_3), 3.12 (3H, s, NCH_3), 3.78 (3H, s, OCH_3), 6.82 (4H, m, ArH on the B-ring), 7.02 (1H, d, J = 2.0 Hz, ArH-3), 7.26 (1H, m, ArH-5), 8.14 (1H, d, J = 8.0, ArH-6). MS m/z (%) 305 (M + 1, 12), 307 (M + 3, 4), 274 (M − 31, 100).

*5.1.8.2. 3-Chloro-5-(N-(4-methoxyphenyl)-N-methylamino)-N-methylbenzamide (**4d**).* Starting with **4a** (61 mg, 0.20 mmol) at 100 °C for 1 h to produce 52 mg of **4d**, 85% yield, white solid, mp 144–145 °C; ^{1}H NMR δ ppm 2.96 (3H, d, J = 4.8 Hz, NCH_3), 3.26 (3H, s, NCH_3), 3.83 (3H, s, OCH_3), 5.96 (1H, s, CONH), 6.73 (1H, s, ArH-2), 6.93 (2H, d, J = 8.8 Hz, ArH-2′,6′), 6.96 (1H, s, ArH-4), 6.99 (1H, s, ArH-6), 7.10 (2H, d, J = 8.8 Hz, ArH-3′,5′). MS m/z (%) 305 (M + 1, 100), 307 (M + 3, 31); HPLC purity 99.3%.

*5.1.8.3. 5-(N-(4-Methoxyphenyl)-N-methylamino)-3-trifluoromethyl-N-methylbenzamide (**4e**).* Starting with **4b** (102 mg, 0.30 mmol) at 100 °C for 1 h to produce 90 mg of **4e** in 89% yield, yellow solid, mp 115–116 °C; ^{1}H NMR δ ppm 2.99 (3H, d, J = 4.8 Hz, NCH_3), 3.31 (3H, s, NCH_3), 3.84 (3H, s, OCH_3), 6.05 (1H, s, CONH), 6.94 (2H, d, J = 8.8 Hz, ArH-2′,6′), 6.97 (1H, s, ArH-2), 7.11 (2H, d, J = 8.8 Hz, ArH-3′,5′), 7.20 (1H, s, ArH-4), 7.26 (1H, s, ArH-6). MS m/z (%) 339 (M + 1, 100); HPLC purity 96.3%.

*5.1.8.4. 3-Bromo-5-(N-(4-methoxyphenyl)-N-methylamino)-N-methylbenzamide (**4f**).* Starting with **4c** (100 mg, 0.29 mmol) at 100 °C for 1 h to produce 82 mg of **4f** in 82% yield, white solid, mp 155–156 °C; ^{1}H NMR δ ppm 2.96 (3H, d, J = 4.4 Hz, NCH_3), 3.26 (3H, s, NCH_3), 3.83 (3H, s, OCH_3), 5.98 (1H, s, CONH), 6.89 (1H, s, ArH-2), 6.93 (2H, d, J = 8.8 Hz, ArH-2′,6′), 7.03 (1H, s, ArH-4), 7.08 (1H, s, ArH-6), 7.10 (2H, d, J = 8.8 Hz, ArH-3′,5′). MS m/z (%) 349 (M + 1, 100), 351 (M + 3, 95); HPLC purity 97.9%.

*5.1.9. 3-Bromo-5-(N-(4-methoxyphenyl)-N-methylamino)-N,N-dimethylbenzamide (**4g**)*

Prepared in the same manner as **3c**. Starting with **4f** (70 mg, 0.20 mmol), methyl iodide (0.02 mL, 0.32 mmol) and NaH (16 mg, 0.40 mmol) to produce 65 mg of **4g**, 90% yield, brown solid, mp 80–81 °C; ^{1}H NMR δ ppm 2.94 (3H, s, NCH_3), 3.05 (3H, s, NCH_3), 3.23 (3H, s, NCH_3), 3.83 (3H, s, OCH_3), 6.61 (1H, dd, J = 1.2 and 1.2 Hz, ArH-4) 6.82 (1H, m, ArH-2), 6.83 (1H, m, ArH-6), 6.92 (2H, d, J = 8.8 Hz, ArH-2′,6′), 7.10 (2H, d, J = 8.8 Hz, ArH-3′,5′). MS m/z (%) 363 (M + 1, 100), 365 (M + 3, 95); HPLC purity 98.4%.

*5.1.10. 3-Bromo-5-(N-(4-methoxyphenyl)-N-methylamino)benzoic acid (**4h**)*

To a solution of **4c** (76 mg, 0.20 mmol) in THF/MeOH (2/2 mL) was added aq NaOH (3 N, 2 mL), and the mixture was heated at

reflux for 5 h. After removal of solvent *in vacuo*, the mixture was poured into ice-water, and the insoluble solid (pH 12) was removed by filtration. The filtrate was acidified to pH 2, until there was no further precipitation. The solid was collected by filtration, washed with water until neutral, and dried to obtain 178 mg of **4h** in 90% yield, yellow solid, mp 242–244 °C; ^{1}H NMR (DMSO-d_6) δ ppm 3.17 (3H, s, NCH_3), 3.77 (3H, s, OCH_3), 7.46 (1H, m, ArH-4), 6.97 (2H, d, J = 8.8 Hz, ArH-2′,6′), 7.11 (2H, d, J = 8.8 Hz, ArH-3′,5′), 7.18 (1H, d, J = 1.2 Hz, ArH-6), 7.31 (1H, s, ArH-2). MS m/z (%) 336 (M + 1, 100), 338 (M + 3, 97).

5.1.11. 3-Bromo-5-(N-(4-methoxyphenyl)-N-methylamino)-N-cyclopropylbenzamide (**4i**)

A mixture of **4h** (105 mg, 0.31 mmol), EDCI (90 mg, 0.47 mmol), and HOBt (64 mg, 0.47 mmol) in CH_2Cl_2 (5 mL) was stirred at rt for 30 min, and then cyclopropylamine (27 mg, 0.47 mmol) was added dropwise at 0 °C with stirring over 15 min, followed by warming to rt for an additional 24 h. The mixture was added to water (20 mL) and extracted with CH_2Cl_2 three times. The combined organic phase was washed with water and brine, successively, and dried over anhydrous Na_2SO_4 overnight. After removal of solvent *in vacuo*, crude product was purified by flash column chromatography (gradient elution: EtOAc/petroleum ether, 0–50%) to give 95 mg of pure **4i** in 82% yield, white solid, mp 184–186 °C; ^{1}H NMR δ ppm 0.59 (2H, m, CH_2), 0.85 (2H, m, CH_2), 2.84 (1H, m, CH), 3.26 (3H, s, NCH_3), 3.83 (3H, s, OCH_3), 6.09 (1H, br, NH), 6.87 (1H, dd, J = 1.6 & 2.0 Hz, ArH-2), 6.93 (2H, d, J = 8.8 Hz, ArH-2′,6′), 7.05 (2H, m, ArH-4,6), 7.09 (2H, d, J = 8.8 Hz, ArH-3′,5′). MS m/z (%) 375 (M + 1, 69), 377 (M + 3, 79), 320 (M - 54, 100); HPLC purity 99.1%.

5.1.12. 3-Bromo-5-(N-(4-methoxyphenyl)-N-methylamino)-N-cyclopentylbenzamide (**4j**)

As for **4i**. Starting with **4h** (168 mg, 0.50 mmol), EDCI (144 mg, 0.75 mmol), HOBt (101 mg, 0.75 mmol), and cyclopentylamine (64 mg, 0.75 mmol) to produce 161 mg of **4j** in 80% yield, white solid, mp 173–174 °C; ^{1}H NMR δ ppm1.46 (2H, m, CH_2), 1.69 (4H, m, 2× CH_2), 2.08 (2H, m, CH_2), 3.26 (3H, s, NCH_3), 3.83 (3H, s, OCH_3), 4.33(1H, m, CH), 5.90 (1H, br, NH), 6.86 (1H, dd, J = 2.0 and 2.0 Hz, ArH-2), 6.93 (2H, d, J = 10.0 Hz, ArH-2′,6′), 7.04 (1H, s, ArH-4), 7.10 (3H, m, ArH-3′,5′,6). MS m/z (%) 403 (M + 1, 100), 405 (M + 3, 91).

5.1.13. N-(3-Chloro-5-carbomethoxy)phenyl-6-methoxy-1,2,3,4-tetrahydroquinoline (**5a**)

Prepared in the same manner as **2b**. Starting with methyl 3-chloro-5-iodobenzoate (297 mg, 1.0 mmol), 6-methoxy-1,2,3,4-tetrahydroquinoline (**7**) (163 mg, 1.0 mmol) at 120 °C for 30 min to produce 255 mg of **5a** in 77% yield, yellow oil; ^{1}H NMR δ ppm 1.96 (2H, m, 3′-CH_2), 2.76 (2H, t, J = 6.4 Hz, 4′-CH_2), 3.61 (2H, t, J = 6.4 Hz, 2′-CH_2), 3.78 (3H, s, OCH_3), 3.89 (3H, s, OCH_3), 6.64 (1H, d, J = 3.2 Hz, ArH-5′), 6.67 (1H, dd, J = 8.8 & 3.2 Hz, ArH-7′), 6.96 (1H, d, J = 8.8 Hz, ArH-8′), 7.28 (1H, m, ArH-6), 7.51 (1H, m, ArH-4), 7.66 (1H, m, ArH-2). MS m/z (%) 332 (M + 1, 100), 334 (M + 3, 30); HPLC purity 97.2%.

5.1.14. N-(3-Bromo-5-carbomethoxy)phenyl-6-methoxy-1,2,3,4-tetrahydroquinoline (**5b**)

Prepared in the same manner as **2d**. Starting with methyl 3,5-dibromobenzoate (294 mg, 1.0 mmol), **7** (179 mg, 1.1 mmol) for 12 h to produce 255 mg of **5b** in 68% yield, yellow oil; ^{1}H NMR δ ppm 1.96 (2H, m, 3′-CH_2), 2.76 (2H, t, J = 6.4 Hz, 4′-CH_2), 3.61 (2H, t, J = 6.4 Hz, 2′-CH_2), 3.78 (3H, s, OCH_3), 3.89 (3H, s, OCH_3), 6.65 (1H, dd, J = 9.2 and 2.8 Hz, ArH-7′), 6.68 (1H, d, J = 2.8 Hz, ArH-5′), 6.95 (1H, d, J = 9.2 Hz, ArH-8′), 7.43 (1H, t, J = 2.0 Hz, ArH-4), 7.66 (1H, t, J = 2.0 Hz, ArH-6), 7.66 (1H, m, ArH-2). MS m/z (%) 376 (M + 1, 100), 378 (M + 3, 91).

5.1.15. N-(3-Chloro-5-(N-methyl)carbamoyl)phenyl-6-methoxy-1,2,3,4-tetrahydroquinoline (**5c**)

Prepared in the same manner as **3d**. Starting with **5a** (100 mg, 0.30 mmol) at 100 °C for 1 h to produce 91 mg of **5c**, 92% yield, pale yellow solid, mp 179–180 °C; ^{1}H NMR δ ppm 1.96 (2H, m, 3′-CH_2), 2.75 (2H, t, J = 6.0 Hz, 4′-CH_2), 2.98 (3H, d, J = 4.8 Hz, NCH_3), 3.61 (2H, t, J = 6.0 Hz, 2′-CH_2), 3.78 (3H, s, OCH_3), 6.05 (1H, bs, NH), 6.68 (2H, m, ArH-5′,7′), 6.97 (1H, d, J = 8.4 Hz, ArH-8′), 7.17 (1H, d, J = 1.6 Hz, ArH-6), 7.20 (1H, d, J = 1.6 Hz, ArH-4), 7.40 (1H, s, ArH-2). MS m/z (%) 331 (M + 1, 100), 333 (M + 3, 32); HPLC purity 99.0%.

5.1.16. N-(3-Bromo-5-(N-methyl)carbamoyl)phenyl-6-methoxy-1,2,3,4-tetrahydroquinoline (**5d**)

Prepared in the same manner as **3d**. Starting with **5b** (64 mg, 0.17 mmol) at 100 °C for 1 h to produce 57 mg of **5d**, 92% yield, white solid, mp 161–162 °C; ^{1}H NMR δ ppm 1.96 (2H, m, 3′-CH_2), 2.75 (2H, t, J = 6.0 Hz, 4′-CH_2), 2.99 (3H, d, J = 4.8 Hz, NCH_3), 3.60 (2H, t, J = 6.0 Hz, 2′-CH_2), 3.78 (3H, s, OCH_3), 6.02 (1H, bs, NH), 6.68 (2H, m, ArH-5′,7′), 6.96 (1H, d, J = 8.4 Hz, ArH-8′), 7.32 (1H, s, ArH-4), 7.36 (1H, s, ArH-6), 7.44 (1H, s, ArH-2). MS m/z (%) 375 (M + 1, 100), 377 (M + 3, 97); HPLC purity 98.2%.

5.1.17. N-(3-Bromo-5-carboxy)phenyl-6-methoxy-1,2,3,4-tetrahydroquinoline (**5e**)

Prepared in the same manner as **4h**. Starting with **5b** (226 mg, 0.60 mmol) to produce 178 mg of **5e** in 82% yield, yellow solid, mp 176–178 °C; ^{1}H NMR δ ppm 1.97 (2H, m, 3′-CH_2), 2.76 (2H, t, J = 6.0 Hz, 4′-CH_2), 3.61 (2H, t, J = 6.0 Hz, 2′-CH_2), 3.79 (3H, s, OCH_3), 6.68 (2H, m, ArH-5′,7′), 6.98 (2H, d, J = 8.8 Hz, ArH-8′), 7.48 (1H, t, J = 2.0 Hz, ArH-6), 7.70 (1H, dd, J = 2.0 and 1.6 Hz, ArH-4), 7.48 (1H, dd, J = 2.0 and 1.6 Hz, ArH-2). MS m/z (%) 362 (M + 1, 100), 364 (M + 3, 72).

5.1.18. N-(3-Bromo-5-(N-cyclopropyl)carbamoyl)phenyl-6-methoxy-1,2,3,4-tetrahydroquinoline (**5f**)

Prepared in the same manner as **4i**. Starting with **5e** (109 mg, 0.30 mmol), EDCI (115 mg, 0.60 mmol), HOBt (81 mg, 0.60 mmol), and cyclopropylamine (56 mg, 1.0 mmol) to produce 108 mg of **5f** in 90% yield, white solid, mp 163–164 °C; ^{1}H NMR δ ppm 0.61 (2H, m, CH_2), 0.86 (2H, m, CH_2), 1.95 (2H, m, 3′-CH_2), 2.75 (2H, t, J = 6.4 Hz, 4′-CH_2), 2.86 (1H, m, CH), 3.60 (2H, t, J = 6.0 Hz, 2′-CH_2), 3.78 (3H, s, OCH_3), 6.12 (1H, br, NH), 6.66 (2H, m, ArH-5′,7′), 6.95 (1H, d, J = 8.4 Hz, ArH-8′), 7.26 (1H, t, J = 2.0 Hz, ArH-4), 7.35 (1H, d, J = 2.0 Hz, ArH-2), 7.43 (1H, t, J = 2.0 Hz, ArH-6); ^{13}C NMR δ ppm 6.91 (CH_2), 23.38 (CH), 23.39 (CH_2), 27.71 (CH_2), 49.78 (CH_2), 55.71 (OCH_3), 112.59 (CH), 114.35 (CH), 117.61 (CH), 120.62 (CH), 121.48 (CH), 123.02 (C), 125.54 (CH), 130 40 (C), 135.66 (C), 137.15 (C), 150.75 (C), 154.51 (C), 167.95 (C), 195.50 (CO). MS m/z (%) 401 (M + 1, 100), 403 (M + 3, 90); HPLC purity 98.4%.

5.1.19. 6-Methoxy-N-(naphthalen-1-yl)-1,2,3,4-tetrahydroquinoline (**6a**)

Prepared in the same manner as **2d**. Starting with 1-bromonaphthalene (206 mg, 1.0 mmol) and **7** (179 mg, 1.1 mmol) for 12 h to produce 196 mg of **6a** in 68% yield, pale yellow solid, mp 93–95 °C; ^{1}H NMR δ ppm 2.15 (2H, br, 3-CH_2), 2.98 (2H, br, 4-CH_2), 3.63 (2H, t, J = 5.6 Hz, 2-CH_2), 3.72 (3H, s, 6-OCH_3), 6.06 (1H, d, J = 8.8 Hz, ArH-8), 6.41 (1H, dd, J = 8.8 & 2.8 Hz, ArH-7), 6.68 (1H, d, J = 2.8 Hz, ArH-5), 6.97 (1H, d, J = 7.2 Hz, ArH-2′), 7.46 (3H, m, ArH-3′,6′,7′), 7.74 (1H, d, J = 8.0 Hz, ArH-4′), 7.89 (1H, d, J = 8.0 Hz, ArH-5′), 8.02 (1H, d, J = 8.0 Hz, ArH-8′). MS m/z (%) 290 (M + 1, 100), 274 (M − 15, 100); HPLC purity 98.2%.

5.1.20. 6-Methoxy-2′-methyl-3,4-dihydro-2H-1,4′-biquinoline (**6b**)

Prepared in the same manner as **2d**. Starting with 4-chloro-2-methylquinoline (178 mg, 1.0 mmol) and **7** (180 mg, 1.1 mmol) for

12 h to produce 228 mg of **6b** in75% yield, yellow solid, mp 120–121 °C; ^{1}H NMR δ ppm 2.03 (2H, m, 3-CH_2), 2.65 (3H, s, 2′-CH_3), 2.94 (2H, t, J = 6.4 Hz, 4-CH_2), 3.71 (2H, t, J = 5.6 Hz, 2-CH_2), 3.77 (3H, s, 6-OCH_3), 6.46 (1H, d, J = 9.2 Hz, ArH-8), 6.53 (1H, dd, J = 9.2 & 2.8 Hz, ArH-7), 6.71 (1H, d, J = 2.8 Hz, ArH-5), 6.97 (1H, s, ArH-3′), 7.38 (1H, m, ArH-6′), 7.64 (1H, m, ArH-7′), 7.90 (1H, d, J = 8.4 Hz, ArH-8′), 8.01 (1H, d, J = 8.4 Hz, ArH-5′); ^{13}C NMR δ ppm 22.41 (CH_2), 25.59 (CH_3), 27.67 (CH_2), 51.39 (CH_2), 55.68 (OCH_3), 112.78 (CH), 114.34 (CH), 116.44 (CH), 120.25 (CH), 123.58 (C), 124.31 (CH), 124.96 (CH), 127.55 (C), 129.27 (CH), 129.50 (CH), 138.14 (C), 149.92 (C), 153.93 (C), 154.75 (C), 159.78 (C). MS m/z (%) 305 (M + 1, 100); HPLC purity 99.3%.

5.1.21. 6-Methoxy-N-(2′-methylquinazol-4′-yl)-1,2,3,4-tetrahydroquinoline (**6c**)

A mixture of 4-chloro-2-methylquinazoline (89 mg, 0.5 mmol), **7** (98 mg, 0.5 mmol), and $NaHCO_3$ (126 mg, 1.5 mmol) in absolute anhydrous EtOH (5 mL) was refluxed for 3 h. The mixture was poured into ice-water, acidified to pH 3 with aq HCl (2 N), and extracted with EtOAc three times. The combined organic phases were washed with water and brine, successively, and dried over anhydrous Na_2SO_4 overnight. After removal of solvent *in vacuo*, the crude product was purified by flash column chromatography (gradient elution: EtOAc/petroleum ether, 0–50%) to obtain 121 mg of pure **6c** in79% yield, yellow solid, mp 134–136 °C; ^{1}H NMR δ ppm 2.11 (2H, m, 3′-CH_2), 2.73 (3H, s, CH_3), 2.88 (2H, t, J = 6.8 Hz, 4′-CH_2), 3.79 (3H, s, OCH_3), 4.05 (2H, t, J = 6.8 Hz, 2′-CH_2), 6.53 (1H, dd, J = 8.8 & 2.8 Hz, ArH-7′), 6.63 (1H, d, J = 8.8 Hz, ArH-8′), 6.78 (1H, d, J = 2.8 Hz, ArH-5′), 7.12 (1H, m, ArH-6), 7.32 (1H, dd, J = 8.4 &1.2 Hz, ArH-5), 7.62 (1H, m, ArH-7), 7.79 (1H, d, J = 8.0 Hz, ArH-8); ^{13}C NMR δ ppm 24.42 (CH_2), 26.65 (CH_3), 27.39 (CH_2), 47.49 (CH_2), 55.62 (OCH_3), 112.00 (CH), 113.70 (CH), 115.68 (C), 122.28 (CH), 124.40 (CH), 126.29 (CH), 128.00 (CH), 132.35 (CH), 132.45 (C), 136.22 (C), 152.43 (C), 156.07 (C), 161.95 (C), 163.99 (C). MS m/z (%) 306 (M + 1, 100); HPLC purity 98.8%.

5.1.22. N-(2′-Chloroquinazol-4′-yl)-6-methoxy-1,2,3,4-tetrahydroquinoline (**6d**)

Similar procedure to that of **6c**. Starting with 2,4-dichloroquinazoline (200 mg, 1.0 mmol), **7** (163 mg, 1.0 mmol), and $NaHCO_3$ (252 mg, 3.0 mmol) in absolute anhydrous EtOH (8 mL) for 3 h to produce 282 mg of **6d** in 87% yield, yellow solid, mp 136–138 °C; ^{1}H NMR δ ppm 2.12 (2H, m, 3′-CH_2), 2.86 (2H, t, J = 6.8 Hz, 4′-CH_2), 3.81 (3H, s, OCH_3), 4.07 (2H, t, J = 6.8 Hz, 2′-CH_2), 6.55 (1H, dd, J = 8.8 and 2.8 Hz, ArH-7′), 6.70 (1H, d, J = 8.8 Hz, ArH-8′), 6.81 (1H, d, J = 2.8 Hz, ArH-5′), 7.13 (1H, m, ArH-6), 7.32 (1H, dd, J = 8.8 and 1.2 Hz, ArH-5), 7.63 (1H, m, ArH-7), 7.78 (1H, dd, J = 8.8 Hz and 1.2 Hz, ArH-8); ^{13}C NMR δ ppm 23.67 (CH_2), 26.84 (CH_2), 48.86 (CH_2), 55.78 (OCH_3), 112.82 (CH), 113.14 (C), 114.06 (CH), 123.21 (CH), 123.99 (CH), 126.68 (CH ×2), 132.44 (C), 135.44 (CH), 135.86 (C), 145.79 (C), 152.50 (C), 159.10 (C), 160.89 (C). MS m/z (%) 326 (M + 1, 100), 328 (M + 3, 31); HPLC purity 98.4%.

5.1.23. 6-Methoxy-N-(2′-(N-methyl)aminoquinazol-4′-yl)-1,2,3,4-tetrahydroquinoline (**6e**)

Prepared in the same manner as **3d**. Staring with **6d** (65 mg, 0.20 mmol) in 3 mL of methylamine (30%) was heated to 100 °C for 1 h to produce 42 mg of **6e** in 66% yield, yellow solid, mp 139–140 °C; ^{1}H NMR δ ppm 2.07 (2H, m, 3′-CH_2), 2.85 (2H, t, J = 6.8 Hz, 4′-CH_2), 3.10 (3H, d, J = 5.2 Hz, NCH_3), 3.79 (3H, s, OCH_3), 3.94 (2H, t, J = 6.8 Hz, 2′-CH_2), 6.53 (1H, dd, J = 9.2 & 2.8 Hz, ArH-7′), 6.67 (1H, d, J = 9.2 Hz, ArH-8′), 6.76 (1H, d, J = 2.8 Hz, ArH-5′), 6.83 (1H, m, ArH-6), 7.29 (1H, d, J = 8.0 Hz, ArH-5), 7.46 (1H, m, ArH-7), 7.52 (1H, d, J = 8.0 Hz, ArH-8). MS m/z (%) 321 (M + 1, 100); HPLC purity 98.6%.

5.2. Antiproliferative activity assay

Target compounds were assayed by the SRB method for cytotoxic activity using a HTCL assay according to procedures described previously [22–24]. The panel of cell lines included human lung carcinoma (A549), epidermoid carcinoma of the nasopharynx (KB), P-gp-expressing epidermoid carcinoma of the nasopharynx (KBvin), and prostate cancer (DU145). The cytotoxic effects of each compound were expressed as GI_{50} values, which represent the molar drug concentrations required to cause 50% tumor cell growth inhibition.

5.3. Tubulin assays

Tubulin assembly was measured by turbidimetry at 350 nm as described previously [25]. Assay mixtures contained 1.0 mg/mL (10 μM) tubulin and varying compound concentrations were pre-incubated for 15 min at 30 °C without guanosine 5′-triphosphate (GTP). The samples were placed on ice, and 0.4 mM GTP was added. Reaction mixtures were transferred to 0 °C cuvettes, and turbidity development was followed for 20 min at 30 °C following a rapid temperature jump. Compound concentrations that inhibited increase in turbidity by 50% relative to a control sample were determined.

Inhibition of the binding of [^{3}H]colchicine to tubulin was measured as described previously [26]. Incubation of 1.0 μM tubulin with 5.0 μM [^{3}H]colchicine and 5.0 μM or 1.0 μM inhibitor was for 10 min at 37 °C, when about 40–60% of maximum colchicine binding occurs in control samples.

5.4. Aqueous solubility

Determination. Solubility was measured at pH 7.4 by using an HPLC–UV method. Test compounds were initially dissolved in DMSO at a concentration of 1.0 mg/mL. Ten microliters of this stock solution were added to pH 7.4 phosphate buffer (1.0 mL) with the final DMSO concentration being 1%. The mixture was stirred for 4 h at rt and then centrifuged at 3000 rpm for 10 min. The saturated supernatants were transferred to other vials for analysis by HPLC–UV. Each sample was performed in triplicate. For quantification, a model 1200 HPLC–UV (Agilent) system was used with an Agilent Eclipse XDB-C18 column (150 mm × 4.6 mm, 5 μm) and elution was with 50%–80% ACN in water. The flow rate was 0.8 mL/min, and injection volume was 20 μL. Aqueous concentration was determined by comparison of the peak area of the saturated solution with a standard curve plotted peak area versus known concentrations, which were prepared by solutions of test compound in ACN at 50, 12.5, 3.13, 0.78, and 0.20 μg/mL.

5.5. Log P measurement

1–2 mg of test compound was dissolved in 1.0–2.0 mL of *n*-octane to obtain a 1.0 mg/mL solution. Next, the same volume of water as *n*-octane was added to each vial. The mixture was stirred at rt for 24 h, and then was left without stirring overnight. The aqueous and organic phases of each mixture were transferred to separate vials for HPLC analysis. The instrument and conditions were the same as those for water solubility determinations. The log P was calculated by the peak area ratio in *n*-octane and in water.

5.6. Microsomal stability assay

Stock solutions of test compounds (1 mg/mL) were prepared by dissolving the pure compound in DMSO, and the solutions were stored at 4 °C. Before assay, the stock solution was diluted with ACN

to 0.1 mM. For measurement of metabolic stability, all compounds were brought to a final concentration of 1 μM with 0.1 M potassium phosphate buffer at pH 7.4, which contained 0.1 mg/mL human liver microsomes and 5 mM $MgCl_2$. The incubation volumes were 300 μL, and reaction temperature was 37 °C. Reactions were started by adding 60 μL of NADPH (final concentration, 1.0 mM) and quenched by adding 600 μL of ice-cold ACN to stop the reaction at 5, 15, 30, and 60 min time points. Samples at the 0 min time point were prepared by adding 600 μL of ice-cold ACN first, followed by 60 μL of NADPH. All samples were prepared in duplicate. After quenching, all samples were centrifuged at 12,000 rpm for 5 min at 0 °C. The supernatant was collected, and 20 μL of the supernatant was directly injected into a Shimadzu LC–MS 2010 system with an electrospray ionization source for further analysis. The following controls were also used: (1) positive control incubation containing liver microsomes, NADPH, reference compound propranolol or terfenadine; (2) negative control incubation omitting NADPH; (3) baseline control containing only liver microsomes and NADPH. The peak heights of test compounds at different time points were converted to percentage of compound remaining, and the peak height values at initial time (0 min) served as 100% values. The slope of the linear regression from log percentage remaining versus incubation time relationships (−k) was used to calculate the *in vitro* half-life ($t_{1/2}$) by the formula of *in vitro* $t_{1/2} = 0.693/k$, regarded as first-order kinetics. Conversion to *in vitro* CL_{int} (in units of mL/min/mg of protein) was calculated by the formula $CL_{int} = [0.693/(\textit{in vitro}\ t_{1/2})][(\text{mL incubation})/(\text{mg of microsomes})]$. The HPLC–MS analysis was carried out on a Shimadzu LC–MS 2010 with an electrospray ionization source. An Alltima C18 column (5 μm, 150 mm × 2.1 mm) was used for HPLC with a gradient elution at a flow rate of 0.2 mL/min. The elution condition was ACN (B) in water (A) at 30% for 0–2 min, 85% for 2–6 min, 100% for 6–9 min and 30% for 9–12 min. The MS conditions were optimized to a detector voltage of +1.7 kV, with acquisition mode selected ion monitoring of the appropriate molecular weights of the test compounds. The curved desolvation line temperature was 250 °C, heat block temperature was 200 °C, and neutralizing gas flow was 1.5 L/min. Samples were injected by an autosampler. Electrospray ionization was operated in positive and negative modes.

5.7. Molecular modeling studies

All molecular modeling studies were performed with Discovery Studio 3.0 (Accelrys, San Diego, USA). The crystal structures of tubulin in complex with DAMA–colchicine (PDB: 1SA0) and with TN16 (PDB: 3HKD) were downloaded from the RCSB Protein Data Bank (http://www.rcsb.org/pdb) for possible use in the modeling study. We selected the structure 1SA0 as our modeling system. CDOCKER was used to evaluate and predict in silico binding free energy of the inhibitors and automated docking. The protein protocol was prepared by several operations, including standardization of atom names, insertion of missing atoms in residues and removal of alternate conformations, insertion of missing loop regions based on SEQRES data, optimization of short and medium size loop regions with Looper Algorithm, minimization of remaining loop regions, calculation of pK, and protonation of the structure. The receptor model was typed with the CHARMm force field. A binding sphere with radius of 8.5 Å was defined through the original ligand (DAMA–colchicine) as the binding site for the study. The docking protocol employed total ligand flexibility, and the final ligand conformations were determined by the simulated annealing molecular dynamics search method set to a variable number of trial runs. The docked ligands (**4i**, **5f**, and **6d**) were further refined using in situ ligand minimization with the Smart Minimizer algorithm by standard parameters. The ligand and its surrounding residues within the above defined sphere were allowed to move freely during the minimization, while the outer atoms were frozen. The implicit solvent model of Generalized Born with Molecular Volume (GBMV) was also used to calculate the binding energies.

Acknowledgments

This investigation was supported by Grants 81120108022 and 30930106 from the Natural Science Foundation of China (NSFC) awarded to Dr. Lan Xie and NIH Grant CA17625-32 from the National Cancer Institute awarded to Dr. K. H. Lee. This study was also supported in part by the Taiwan Department of Health, China Medical University Hospital Cancer Research Center of Excellence (DOH100-TD-C-111-005).

Appendix A. Supplementary data

Supplementary data associated with this article can be found in the online version, at http://dx.doi.org/10.1016/j.ejmech.2013.06.041. These data include MOL files and InChiKeys of the most important compounds described in this article.

References

[1] M.A. Jordan, L. Wilson, Microtubules as a target for anticancer drugs, Nat. Rev. Cancer 4 (2004) 253–265.
[2] C. Dumontet, M.A. Jordan, Microtubule-binding agents: a dynamic field of cancer therapeutics, Nat. Rev. Drug Discov. 9 (2010) 790–803.
[3] S. Sengupta, S.A. Thomas, Drug target interaction of tubulin-binding drugs in cancer therapy, Expert Rev. Anticancer Ther. 6 (2006) 1433–1447.
[4] D.W. Siemann, The unique characteristics of tumor vasculature and preclinical evidence for its selective disruption by tumor-vascular disrupting agents, Cancer Treat. Rev. 37 (2011) 63–74.
[5] R.P. Mason, D. Zhao, L. Liu, L. Trawick, K.G. Pinney, A perspective on vascular disrupting agents that interact with tubulin: preclinical tumor imaging and biological assessment, Integr. Biol. 3 (2011) 375–387.
[6] X.F. Wang, X.T. Tian, E. Ohkoshi, B.J. Qin, Y.N. Liu, P.C. Wu, H.Y. Hung, M.J. Hour, K. Qian, R. Huang, K.F. Bastow, W.P. Janzen, J. Jin, S.L. Morris-Natschke, K.H. Lee, L. Xie, Design and synthesis of diarylamines and diarylethers as cytotoxic antitumor agents, Bioorg. Med. Chem. Lett. 22 (2012) 6224–6228.
[7] X.F. Wang, E. Ohkoshi, S.B. Wang, E. Hamel, K.F. Bastow, S.L. Morris-Natschke, K.H. Lee, L. Xie, Synthesis and biological evaluation of *N*-alkyl-*N*-(4-methoxyphenyl)pyridin-2-amines as a new class of tubulin polymerization inhibitors, Bioorg. Med. Chem. 21 (2013) 632–642.
[8] J. Blagg, Structure–activity relationships for *in vitro* and *in vivo* toxicity, in: W. Anthony (Ed.), Annual Reports in Medicinal Chemistry, vol. 41, Academic Press, 2006, pp. 353–368.
[9] E.H. Kerns, L. Di, Metabolic stability, in: In Drug-like Properties: Concepts, Structure Design and Methods, Academic Press, San Diego, 2008, p. 151.
[10] X. Mei, A.T. August, C. Wolf, Regioselective copper-catalyzed amination of chlorobenzoic acids: synthesis and solid-state structures of *N*-aryl anthranilic acid derivatives, J. Org. Chem. 71 (2006) 142–149.
[11] T.A. Jensen, X. Liang, D. Tanner, N. Skjaerbaek, Rapid and efficient microwave-assisted synthesis of aryl aminobenzophenones using Pd-catalyzed amination, J. Org. Chem. 69 (2004) 4936–4947.
[12] V. Onnis, M.T. Cocco, V. Lilliu, C. Congiu, Synthesis and evaluation of antitumor activity of ester and amide derivatives of 2-arylamino-6-trifluoromethyl-3-pyridinecarboxylic acids, Bioorg. Med. Chem. 16 (2008) 2367–2378.
[13] A. Nose, T. Kudo, Reduction of heterocyclic compounds. II. Reduction of heterocyclic compounds with sodium borohydride-transition metal salt systems, Chem. Pharm. Bull. 32 (1984) 2421–2425.
[14] M. Perez-Sayans, J.M. Somoza-Martin, F. Barros-Angueira, P.G. Diz, J.M. Rey, A. Garcia-Garcia, Multidrug resistance in oral squamous cell carcinoma: the role of vacuolar ATPases, Cancer Lett. 295 (2010) 135–143.
[15] H.Y. Hung, E. Ohkoshi, M. Goto, K.F. Bastow, K. Nakagawa-Goto, K.H. Lee, Antitumor agents. 293. Nontoxic dimethyl-4,4′-dimethoxy-5,6,5′,6′-dimethylenedioxylbiphenyl-2,2′-dicarboxylate (DDB) analogues chemosensitize multidrug-resistant cancer cells to clinical anticancer drugs, J. Med. Chem. 55 (2012) 5413–5424.
[16] L.V. Rubinstein, R.H. Shoemaker, R.M. Paull, S. Tosini, P. Skehan, D.A. Scudiero, A. Monks, M.R. Boyd, Comparison of *in vitro* anticancer-drug-screening data generated with a tetrazolium assay versus a protein assay against a diverse panel of human tumor cell lines, J. Natl. Cancer Inst. 82 (1990) 1113–1117.
[17] R.B.G. Ravelli, B. Gigant, P.A. Curmi, I. Jourdain, S. Lachkar, A. Sobel, M. Knossow, Insight into tubulin regulation from a complex with colchicine and a stathmin-like domain, Nature 428 (2004) 198–202.

[18] A. Dorleans, B. Gigant, R.B.G. Ravelli, P. Mailliet, V. Mikol, M. Knossow, Variations in the colchicine-binding domain provide insight into the structural switch of tubulin, Proc. Natl. Acad. Sci. U. S. A. 106 (2009) 13775–13779.
[19] A. Gangjee, Y. Zhao, L. Lin, S. Raghavan, E.G. Roberts, A.L. Risinger, E. Hamel, S.L. Mooberry, Synthesis and discovery of water-soluble microtubule targeting agents that binding to the colchicine site on tubulin and circumvent Pgp medicated resistance, J. Med. Chem. 53 (2010) 8116–8128.
[20] L.Q. Sun, L. Zhu, K. Qian, B. Qin, L. Huang, C.H. Chen, K.H. Lee, L. Xie, Design, synthesis, and preclinical evaluations of novel 4-substituted 1,5-diarylanilines as potent HIV-1 non-nucleoside reverse transcriptase inhibitor (NNRTI) drug candidates, J. Med. Chem. 55 (2012) 7219–7229.
[21] S.X. Cai, Small molecule vascular disrupting agents: potential new drugs for cancer treatment, Anti-Cancer Drugs 2 (2007) 79–101.
[22] M.R. Boyd, Status of the NCI preclinical antitumor drug discovery screen, in: V.T. Devita, S. Hellman, S.A. Rosenberg (Eds.), Cancer: Principles and Practice of Oncology Updates, J. B. Lippincott, Philadelphia, 1989, pp. 1–12.
[23] A. Monks, D. Scudiero, P. Skehan, R. Shoemaker, K. Paull, D. Vistica, C. Hose, J. Langley, P. Cronise, A. Vaigro-Woiff, M. Gray-Goodrich, H. Campbell, J. Mayo, M. Boyd, Feasibility of a high-flux anticancer drug screen using a diverse panel of cultured human tumor cell lines, J. Natl. Cancer Inst. 83 (1991) 757–766.
[24] P. Houghton, R. Fang, I. Techatanawat, G. Steventon, P.J. Hylands, C.C. Lee, The sulphorhodamine (SRB) assay and other approaches to testing plant extracts and derived compounds for activities related to reputed anticancer activity, Methods 42 (2007) 377–387.
[25] E. Hamel, Evaluation of antimitotic agents by quantitative comparisons of their effects on the polymerization of purified tubulin, Cell Biochem. Biophys. 38 (2003) 1–22.
[26] C.M. Lin, H.H. Ho, G.R. Pettit, E. Hamel, Antimitotic natural products combretastatin A-4 and combretastatin A-2: studies on the mechanism of their inhibition of the binding of colchicine to tubulin, Biochemistry 28 (1989) 6984–6991.